Thermal Performance Benchmarking

Annual Report

Gilbert Moreno

NREL is a national laboratory of the U.S. Department of Energy
Office of Energy Efficiency & Renewable Energy
Operated by the Alliance for Sustainable Energy, LLC

This report is available at no cost from the National Renewable Energy Laboratory (NREL) at www.nrel.gov/publications.

Management Report
NREL/MP-5400-64941
April 2016

Contract No. DE-AC36-08GO28308

NREL
NATIONAL RENEWABLE ENERGY LABORATORY

Thermal Performance Benchmarking

Annual Report

Gilbert Moreno

Prepared under Task No. VTP2.7101

NREL is a national laboratory of the U.S. Department of Energy
Office of Energy Efficiency & Renewable Energy
Operated by the Alliance for Sustainable Energy, LLC

This report is available at no cost from the National Renewable Energy Laboratory (NREL) at www.nrel.gov/publications.

National Renewable Energy Laboratory
15013 Denver West Parkway
Golden, CO 80401
303-275-3000 • www.nrel.gov

Management Report
NREL/MP-5400-64941
April 2016

Contract No. DE-AC36-08GO28308

Cover Photos by Dennis Schroeder: (left to right) NREL 26173, NREL 18302, NREL 19758, NREL 29642, NREL 19795.

NREL prints on paper that contains recycled content.

I. Thermal Performance Benchmarking

Principal Investigator: Gilbert Moreno
National Renewable Energy Laboratory (NREL)
Transportation and Hydrogen Systems Center
15013 Denver West Parkway
Golden, CO 80401
Phone: 303-275-4450
E-mail: gilbert.moreno@nrel.gov

DOE Technology Development Manager: Susan A. Rogers
U.S. Department of Energy
1000 Independence Ave. SW EE-3V
Washington, DC 20585
Phone: 202-586-8997
E-mail: susan.rogers@ee.doe.gov

NREL Task Leader: Sreekant Narumanchi
Phone: 303-275-4062
Email: sreekant.narumanchi@nrel.gov

Abstract

The goal for this project is to thoroughly characterize the performance of state-of-the-art (SOA) in-production automotive power electronics and electric motor thermal management systems. Information obtained from these studies will be used to:

- Evaluate advantages and disadvantages of different thermal management strategies
- Establish baseline metrics for the thermal management systems
- Identify methods of improvement to advance the SOA
- Increase the publicly available information related to automotive traction-drive thermal management systems
- Help guide future electric drive technologies (EDT) research and development (R&D) efforts.

The performance results combined with component efficiency and heat generation information obtained by Oak Ridge National Laboratory (ORNL) may then be used to determine the operating temperatures for the EDT components under drive-cycle conditions. In FY15, the 2012 Nissan LEAF power electronics and electric motor thermal management systems were benchmarked. Testing of the 2014 Honda Accord Hybrid power electronics thermal management system started in FY15 and the results will be reported in FY16.

The focus of this project is to benchmark the thermal aspects of the systems. ORNL's benchmarking reports of electric and hybrid electric vehicle technology provide detailed descriptions of the electrical and packaging aspects of these automotive systems [1, 2].

Accomplishments

- We experimentally characterized the thermal performance of the 2012 Nissan LEAF motor and power electronics thermal management systems.
- We developed and validated steady-state and transient thermal models of the 2012 Nissan LEAF motor and power electronics systems. The models were used to identify the thermal bottlenecks within each system. Solutions to improve the thermal performance were proposed.

- We are working to understand heat loss distributions within each system. Heat loss information will be used as inputs into the transient models and used to compute component temperatures under drive-cycle operations.
- We initiated tests to measure the thermal performance of the 2014 Honda Accord power electronics thermal management system.

Introduction

This project will seek out the SOA power electronics and electric motor technologies to benchmark their thermal performance. The benchmarking will focus on the thermal aspects of the system. System metrics including the junction-to-coolant thermal resistance, winding-to-coolant thermal resistance, and the parasitic power consumption of the heat exchangers will be measured. The type of heat exchanger (i.e., channel flow, brazed, folded-fin) and any enhancement features will be identified and evaluated to understand their effect on performance. Additionally, the thermal resistance/conductivity of select power module and motor components will also be measured. The research conducted will allow insight into the various cooling strategies to understand which heat exchangers are most effective in terms of thermal performance and efficiency. Modeling analysis and fluid-flow visualization may also be carried out to better understand the heat transfer and fluid dynamics of the systems. The research conducted will allow insight into the various cooling strategies to understand the current SOA in thermal management for automotive power electronics and electric motors.

Approach

Hardware testing and modeling analyses were conducted to benchmark the performance of the power electronics and electric motor thermal management systems. The project approach is outlined below.

- Collaborate with industry and ORNL to identify the vehicle system to benchmark
  - The 2012 Nissan LEAF power electronics and electric motor thermal management systems were benchmarked in 2015. Tests were initiated to measure the thermal performance of the 2014 Honda Accord Hybrid power electronics thermal management system.
- Experimentally measure the performance of the thermal management systems
  - Measure the power electronics junction-to-liquid and the motor winding-to-liquid thermal resistances
  - Measure the thermal properties of the system components (e.g., thermal pads, stator laminations, motor windings)
  - Measure heat exchanger thermal resistance, pressure drop, volume, and weight
- Create thermal models of the thermal management systems
  - Validate the models using experimental results
  - Compute thermal resistances that cannot be experimentally measured
  - Create transient thermal models and use them to estimate component temperatures under various drive-cycles
- Analyze and report data
  - Identify thermal bottlenecks in the systems and provide solutions to improve the SOA
  - Establish baseline metrics for the thermal management systems
  - Share results with industry and research institutions
  - Support other EDT projects (power electronics thermal management R&D, electric motor thermal management R&D, benchmarking electric vehicle and hybrid electric vehicle technologies [ORNL]).

Results and Discussion

In FY15, the 2012 Nissan LEAF power electronics and electric motor thermal management systems were benchmarked. Experimental testing of the hardware was first completed to measure thermal resistance values of the systems. The laboratory tests were intended to provide an accurate means of measuring thermal performance of the systems and were not intended to simulate actual automotive operating conditions. Steady-state and transient models were then created that were validated against the experimental data. The validated thermal models were used to further understand the heat transfer mechanisms within the systems. The goal is to use the models to compute component temperatures under drive-cycle conditions. Efforts to benchmark the 2014 Honda Accord Hybrid power electronics thermal management system started in FY15.

2012 Nissan LEAF Motor Thermal Management System

Figure 1 shows a picture of the 2012 Nissan LEAF motor. The motor is an interior permanent magnet synchronous machine that outputs a maximum of 80 kW [3]. The motor uses a distributed winding stator configuration. Figure 1 also shows the thermal management system that consists of a water-ethylene glycol (WEG) cooling jacket that is pressed around the motor stator. The cooling jacket is fabricated out of aluminum and has three relatively large coolant channels. The coolant channels have approximate dimensions of 35 mm in width and 12.5 mm in height. The cooling jacket has an inner diameter of approximately 200 mm, an outer diameter of approximately 250 mm, and a total axial length of approximately 210 mm. The approximate weight of the coolant jacket (not including the stator and rotor) is 10.1 kg.

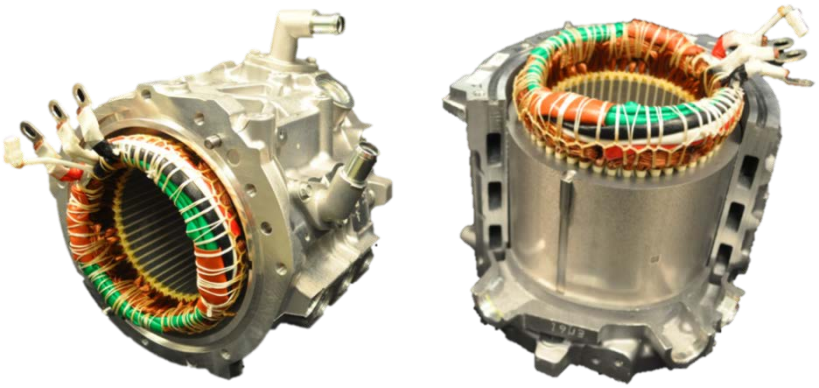

Figure I-1: Pictures of the 2012 Nissan LEAF motor. Image on the right shows the cooling jacket sectioned-off to reveal the internal coolant channels.
Photo Credit: Kevin Bennion (NREL)

Experiments were conducted to measure the thermal performance of the motor thermal management system. For this, the motor was first connected to the WEG flow test bench. The test bench circulated WEG (50%/50% mixture by volume of water and ethylene glycol) at an inlet temperature of 65°C through the cooling jacket. The system thermal resistances were measured at various WEG flow rates. Three direct-current, high-current and low-voltage power supplies were used to provide heating to the motor's windings. Approximately 160 amps were conducted through all three phases of the motor to provide approximately 530 W of total heat. Voltage drop measurements taken at the positive and negative (neutral) sides of each phase were used along with the current supplied to compute the power dissipated. The motor was insulated on all sides with thick layers of insulation to minimize thermal losses to the surrounding environment.

Calibrated K-type thermocouples were installed on various parts of the motor to measure the temperatures at different locations (Figure 2). Twenty thermocouples were installed on the end-windings (both sides) to measure the inner, outer, and axial end-winding surface temperatures. Ten thermocouples were installed on the stator to measure the surface temperatures of the inner stator, slot liner, and interface between the slot liner and stator laminations. The stator surface temperatures were taken on both sides and at the midpoint of the stator. Ten thermocouples were instrumented on the various locations on the cooling jacket.

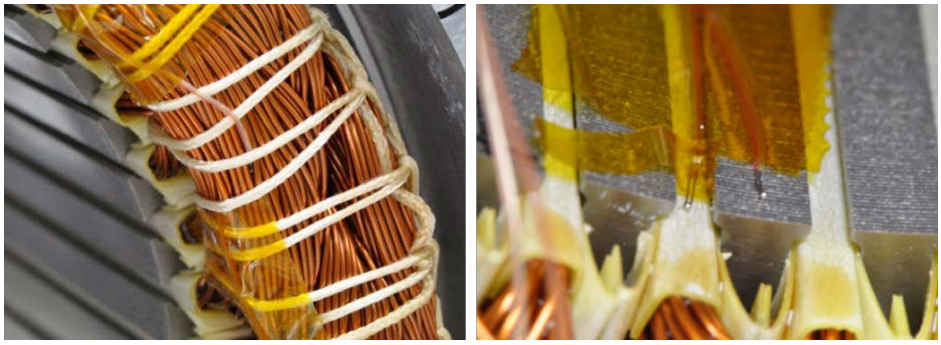

Figure I-2: Pictures show the thermocouple placements on the end-windings (left) and stator surfaces (right).
Photo Credit: Gilbert Moreno (NREL)

Heat balances were calculated for the system to compare total heat generated to the heat absorbed by the WEG at different flow rates. Calculations revealed that heat losses to the surrounding conditions are approximately 9.9% at 1.8 Lpm and decrease to approximately 4.4% at 12 Lpm.

The thermal resistances of the motor were used to quantify the thermal performance of the system. The end-winding-to-liquid thermal resistance was defined using Eq. (1).

$$R_{th,\ w-l} = \frac{(\overline{T_w} - \overline{T_l})}{Q_{Total}} \qquad \text{Equation 1}$$

where $\overline{T_w}$ is the average end-winding temperature, $\overline{T_l}$ is the average WEG temperature, and Q_{Total} is the total heat absorbed by the WEG. The stator-to-liquid thermal resistance was defined using Eq. (2).

$$R_{th,\ s-l} = \frac{(\overline{T_s} - \overline{T_l})}{Q_{Total}} \qquad \text{Equation 2}$$

where $\overline{T_s}$ is the average stator inner-surface temperature.

The measured thermal resistances versus the WEG flow rate for both the end winding and stator are provided in Figure 3. The resistance values are average values based on test repetitions. Figure 3 provides both the thermal resistance (Rth) and the specific thermal resistance (R"th) values. The stator-to-cooling jacket contact area was used to scale the thermal resistance values into a specific thermal resistance (R"th) metric. The specific thermal resistance is a metric that takes into account the size of the motor and its cooling system and can be used when comparing the performance of different motors.

As shown in Figure 3, at WEG flow rates ≥ 4 Lpm, the winding and stator thermal resistances decrease minimally as flow rates increase. This behavior indicates that the passive stack is the dominant thermal resistance at the higher flow rates (≥ 4 Lpm)—significantly greater than the convective resistance. Additionally, higher thermal resistances are measured on the electrical connection side of the motor (side 1). Higher thermal resistances on the electrical connection side of the motor (side 1) are associated with the geometry of the motor (e.g., motor is not perfectly symmetric) and also due to the added heat from the electrical connections.

Computational fluid dynamics (CFD) analysis and finite element analysis (FEA) were also conducted to model the thermal performance of the system. CFD simulations were carried out to model the WEG flow within the cooling channels. Figure 4 shows CFD-generated WEG velocities and coolant channel temperatures. Average heat transfer coefficients were obtained from the CFD analyses at various flow rates and used as boundary conditions in an FEA model (Figure 5). The FEA conditions were identical to the experiments conditions (dissipate approximately 530W through windings via volumetric heat generation). Motor component properties listed in Table 1 and contact thermal resistances listed in Table 2 were used in the model. The work conducted to measure component properties (excluding aluminum) and interface contact resistance was carried out under the EDT Electric Motor Thermal Management R&D Project. The thermal contact resistances provided in Table 2 are preliminary estimates. Work is currently underway to further validate these thermal contact resistance values.

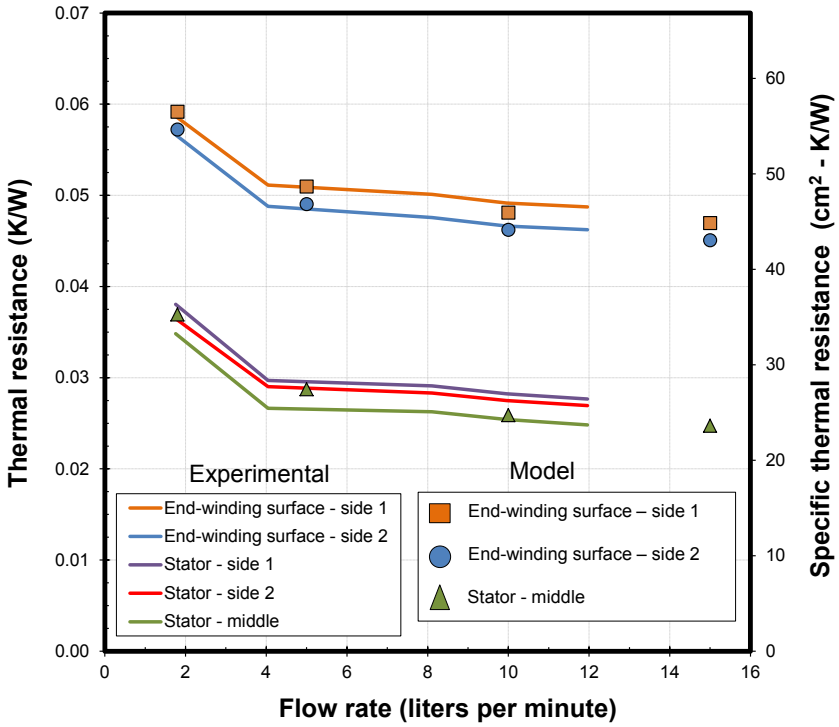

Figure I-3: Experimentally measured and model-predicted thermal resistance values for different parts of the 2012 Nissan LEAF motor stator. Note: Side 1 refers to the end-winding side of the motor that has the electrical connections.

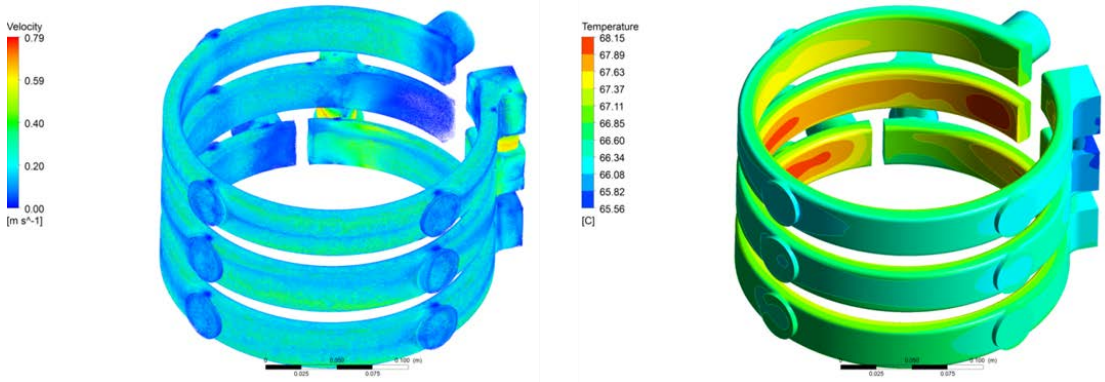

Figure I-4: CFD-generated plots showing the coolant velocities (left) and coolant channel temperatures (right).

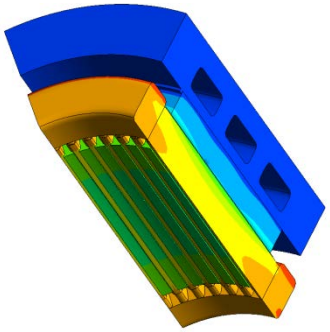

Figure I-5: FEA-generated temperature contours of a one-eighth model of the motor stator.

Table I-1: Thermal conductivity values used in the Nissan LEAF motor stator thermal models.

	Thermal conductivity		
	Radial (W/m-K)	Angular (W/m-K)	Axial (W/m-K)
Laminations [4]	21.9	21.9	1.7
Slot windings	0.99	0.99	292
End windings [5]	0.76	201.7	102
Slot liner	0.18	0.18	0.18
Aluminum [6]	167	167	167

The CFD and FEA predicted winding and stator thermal resistance values are shown as symbols in Figure 3. CFD-estimated average wetted surface heat transfer coefficient values are provided in Table 3. As shown, the model-predicted thermal resistance results provide a good match with the experimentally obtained data, which validates the measured component thermal property and contact resistance values listed in Tables 1 and 2. It is also worth noting that the models capture the sharp increase in the thermal resistance values at the lowest flow rate.

The model was then used to compute a temperature profile from the inner slot liner surface to the coolant. The temperature profile, shown in Figure 6, was used to identify the major thermal bottlenecks within the stator. Figure 6 shows that the passive stack components (from the slot liner to the stator-to-cooling jacket interface) are the dominant thermal resistance within the stator. Moreover, the slot winding-to-stator interface was found to provide the largest thermal bottleneck within the passive stack. Therefore, improving thermal performance of the motor would require improving the contact resistance between the slot windings and the slot liner and between the slot liner and the stator surface. Increasing the thermal conductivity of the resin and improving the resins ability to bond the slot liner to the stator surface should reduce this thermal resistance.

Table I-2: Thermal resistance values used for the Nissan LEAF motor stator thermal models

	Thermal Resistance (mm^2-K/W)
Slot liner to stator	608
Slot winding to slot liner	1,800

Table I-3: CFD-predicted average heat transfer coefficient values for the Nissan LEAF motor cooling jacket

Flow Rate	Channel Velocity (Average)	Heat Transfer Coefficient
Lpm	m/s	W/m^2-K
1.8	0.07	350
5	0.19	803
10	0.39	1,428
15	0.58	2,049

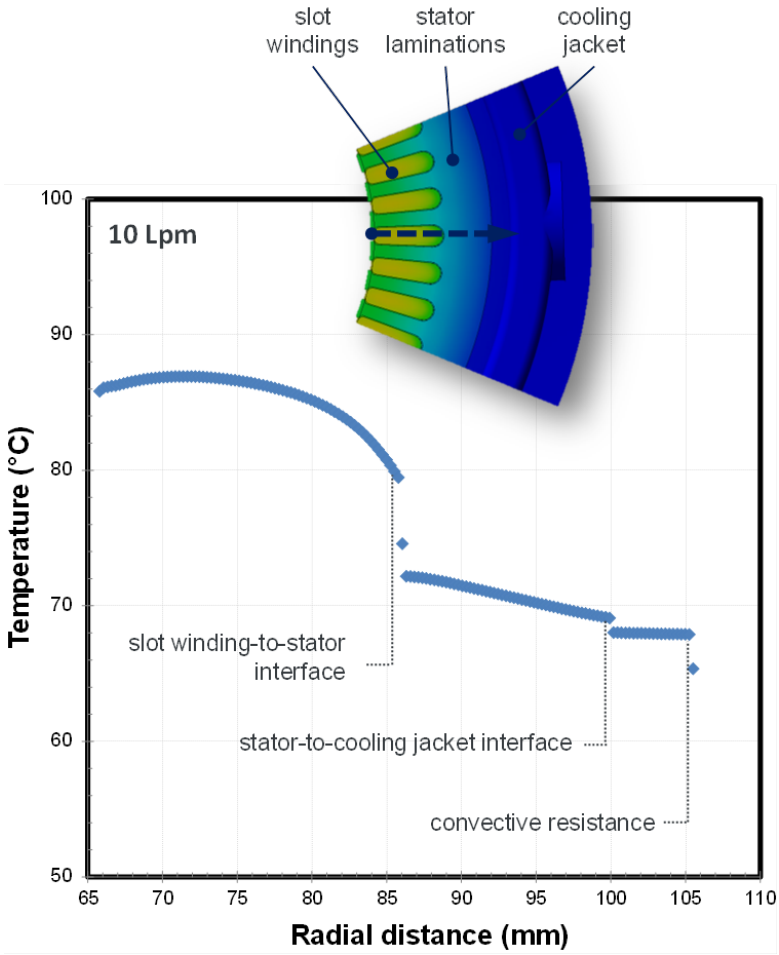

Figure I-6: Temperature profile through the motor stator depicting the thermal path from the inner surface of the slot liner to the coolant. The arrow in the upper image indicates the thermal path.

2012 Nissan LEAF Power Electronics (Inverter) Thermal Management System

Figure 7 shows pictures of the Nissan LEAF power electronics and cooling system. The system consists of three power modules that are mounted onto a cast-aluminum cold plate and associated electronic components (e.g., capacitors, electrical boards, and interconnects). The cold plate is integrated into the inverter housing and weighs approximately 5 kg (not including the top or bottom inverter cover plates). The cold plate cools the power electronics modules by circulating WEG through a series of serpentine fin channels. Figure 8 shows a computer-aided design (CAD) rendering of a LEAF power module. The power modules consist of three insulated gate bipolar transistor (IGBT)-diode pairs per switch position. The cross-sectional view shown in Figure 8 provides a detailed view of the power module layers and interfaces. Unlike most power modules, the LEAF module does not use metalized-ceramic substrates (e.g., direct-bond copper substrates) for electrical isolation. Instead, the LEAF modules incorporate a dielectric pad mounted between the power modules and the cold plate for electrical isolation (Figure 7). Thermal interface material (TIM) is applied on both sides of the dielectric pad to reduce thermal contact resistance.

Tests were conducted to measure the junction-to-coolant resistance for the power modules. For the tests, the inverter was connected to the WEG flow test bench. The test bench circulated WEG (50%/50% of water and ethylene glycol by volume) at a 65°C inlet temperature through the inverter cold plate at various flow rates. The tests were repeated to ensure repeatable results. A transient thermal tester (T3ster) system was used to power/heat and measure the temperature of one IGBT. A total of 50 amps were provided to power one IGBT (approximately 55 W of heat). Measuring temperatures required calibrating the voltage drop through the IGBT to its temperature. Temperature calibration was carried out within a temperature-controlled chamber. Two calibrated K-type thermocouples were mounted onto the power modules (placed near the IGBT that was to be tested) and used to obtain the temperature versus IGBT voltage drop relationship while supplying a 1-milliamp sense current through the device. Ten volts were used to gate the IGBT. The entire system was insulated with thick layers of insulation to minimize thermal losses to the surrounding environment.

Figure 9 shows the experimentally measured junction-to-coolant specific thermal resistance values at different WEG flow rates. The specific thermal resistance was defined per Equation 3:

$$R''_{th,\ j-l} = \frac{(\overline{T_J} - \overline{T_l})}{Q_{Total}} \times A_{IGBT} \qquad \text{Equation 3}$$

where $\overline{T_j}$ is the average junction temperature, $\overline{T_l}$ is the average WEG temperature, Q_{Total} is the total heat dissipated through the IGBT, and A_{IGBT} is the area of the IGBT (225 mm^2).

Figure I-7: Pictures of the 2012 Nissan LEAF inverter. The middle image shows the cold plate cooling channels. Image on the right shows one power module mounted on the cold plate. The dielectric pad and TIM layers are shown (right).
Photo Credit: Gilbert Moreno (NREL)

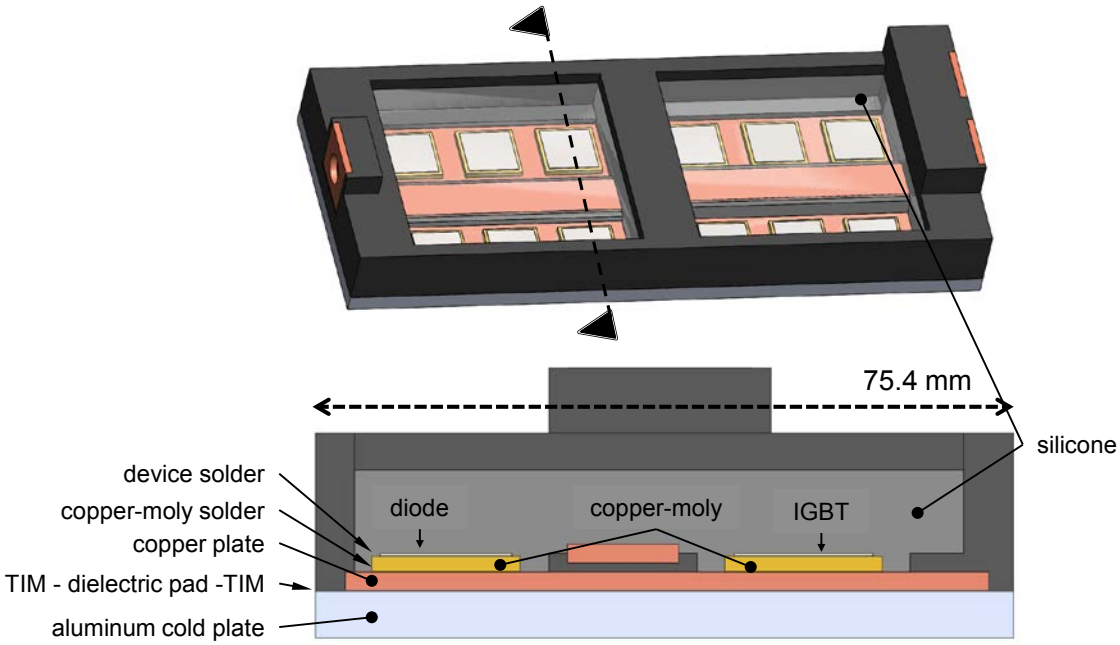

Figure I-8: CAD model of a Nissan LEAF power module. The various power module layers are shown in the lower, cross-sectional view.

The results in Figure 9 show that varying the flow rate has minimal effect on the thermal resistance values. The results indicate that the passive stack thermal resistance is significantly larger than convective resistance (at the flow rates tested). At the typical automotive power electronic flow rates (~10 Lpm) the junction-to-coolant specific thermal resistance is about 79 mm^2-K/W.

CFD and FEA were then used to model the power electronics thermal management systems to better understand the heat transfer within inverter (Figure 10). Table 4 lists the properties, of the various power module components, that were used in the models. Temperature dependent thermal conductivity properties were used for silicon and copper. The thermal conductivity of the dielectric pad was measured using NREL's ASTM TIM stand. The thermal conductivities of the other components were obtained from literature. The composition (e.g., copper-moly, solder, TIM) and thickness of some materials were selected so that the model results provided a good match with experimental data. CFD-computed wetted-surface average heat transfer coefficients are provided in Table 5. The estimated heat transfer coefficient values are relatively low.

The computed heat transfer coefficient values were imposed as boundary conditions in an FEA model. The FEA model replicated the experimental conditions (dissipate approximately 55W through one IGBT). Figure 9 provides the model-estimated maximum (computed using the maximum junction temperature) and average (computed using the average junction temperature) thermal resistance values. As shown, the model-predicted results provide a good match with the experimental data (maximum ~6% difference between model and experimental results). The model was then used to generate a temperature profile from the IGBT to the coolant to identify the largest thermal bottlenecks in the system. The temperature profile is shown in Figure 11 and clearly shows that the passive stack provides the largest thermal bottleneck within the system. The TIM-dielectric pad-TIM interfaces are found to provide the largest resistance within the passive stack. An analysis conducted in the EDT Power Electronics Thermal Management R&D project reveals that 2012 LEAF power module design provides lower steady-state thermal performance (i.e., higher thermal resistance) as compared with more traditional power module configurations (e.g., power modules that incorporate metalized ceramic substrates). However, the LEAF power module design may provide cost and reliability advantages over the traditional power module design. Additionally, the LEAF design may also offer advantages under some transient conditions.

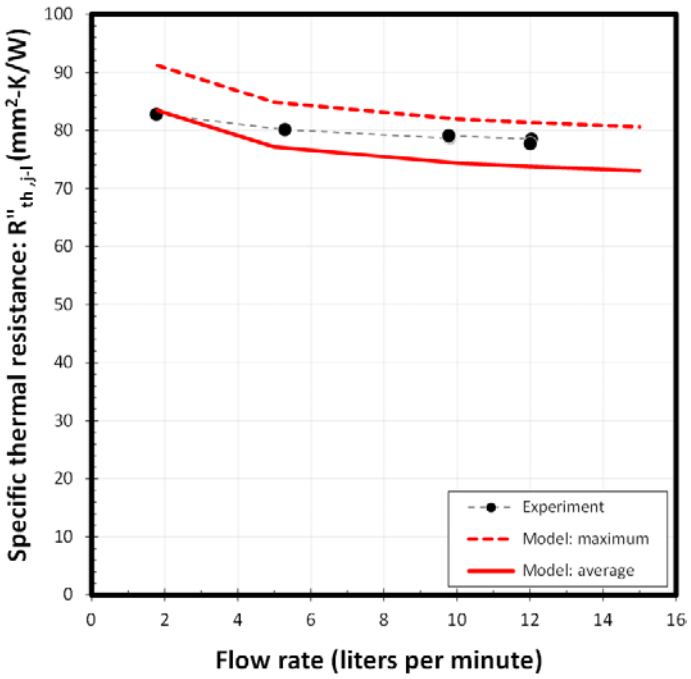

Figure I-9: Experimentally measured and model-predicted IGBT thermal resistance values for the 2012 Nissan LEAF inverter

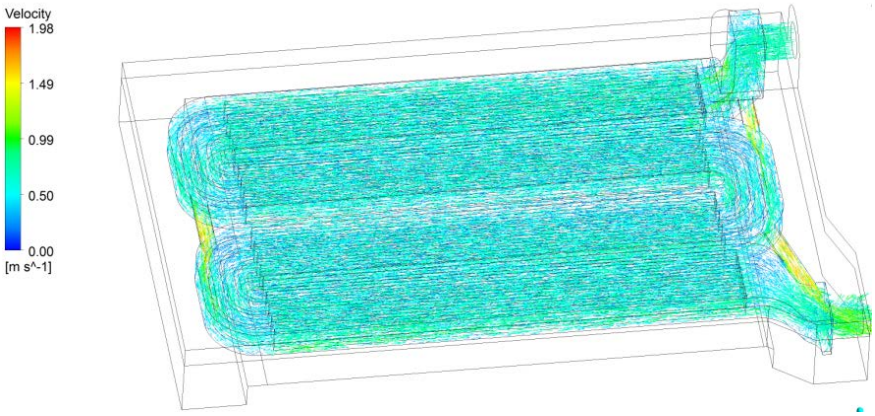

Figure I-10: CFD-generated plot showing the coolant velocity vectors at a flow rate of 10 Lpm

Table I-4: Thermal conductivity and thickness values used in the LEAF inverter thermal models

	Silicon	Solder	Copper-Moly (20-80)	Copper	Plastic	Silicone	Dielectric pad	Aluminum	TIM
Thermal conductivity (W/m-K)	k versus T	35	160	k versus T	0.34	0.68	2.59	167	1
Thickness (mm)	0.25	0.08 (die-attach), 0.04 (copper-moly attach)	1.6	2	N/A	N/A	0.3	3.25	0.08

Table I-5: CFD-predicted average heat transfer coefficient values for the Nissan LEAF inverter cold plate

Flow rate (Lpm)	Heat Transfer Coefficient (W/m^2-K)
1.8	376
5	899
10	1,664
12	1,934
15	2,394

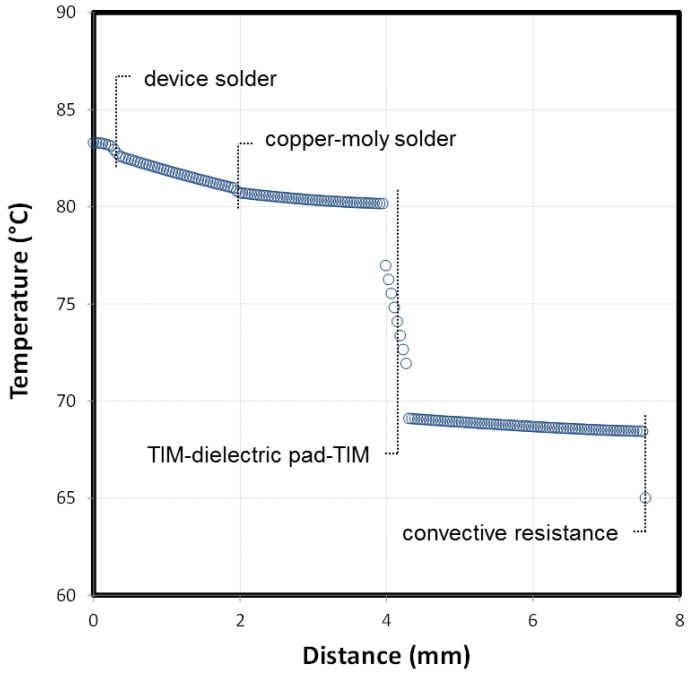

Figure I-11: Temperature profile through the inverter depicting the thermal path from the IGBT to the coolant. The TIM-dielectric pad-TIM layers constitute a significant thermal resistance to the power modules.

Heat Exchanger Parasitic Power versus Flow Rate

Figure 12 plots the experimentally-measured parasitic power versus the flow rate curves for the LEAF motor and power electronics heat exchangers. The motor heat exchanger provided lower pressure drop due to its relatively large coolant channels. This information combined with thermal performance results will be used to compute performance metrics that incorporate the system efficiency.

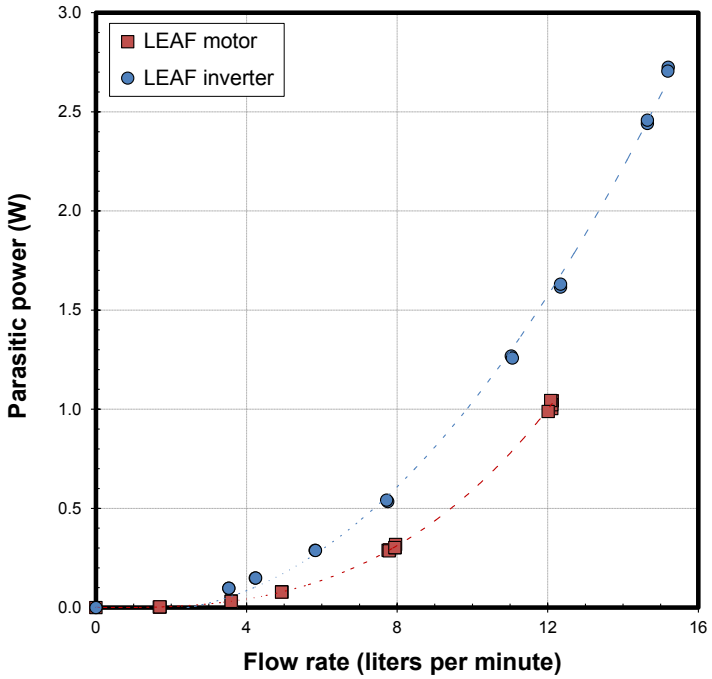

Figure I-12: Experimentally measured parasitic power losses for the Nissan LEAF motor and inverter heat exchangers

Transient Models

Transient FEA models were also created for both the 2012 LEAF motor and power electronics thermal management systems. The transient model results were found to provide a good match to experimentally measured transient results; however, work is currently underway to refine the models to improve their accuracy. The LEAF power module transient modeling results have also been used to generate resistance-capacitance thermal network models that can be used to quickly compute the thermal response of these components under different operating conditions. The goal is to use the various models to predict motor and power electronics component temperatures under drive-cycle operations. We are currently working with ORNL to understand heat-loss distributions within each system. The heat-loss distribution information can be imposed into the models to estimate component temperatures under drive-cycle conditions.

Conclusions and Future Directions

- Experiments were conducted to measure the thermal performance of the 2012 Nissan LEAF motor and power electronics thermal management systems. CFD and FEA thermal models were developed for both systems. The models were found to provide a good match with experimentally obtained data. Experimental and modeling results demonstrate that the passive-stack is the dominant thermal resistance for both the motor and power electronics systems.
- Modeling results indicate that the slot winding-to-stator lamination interface is the greatest thermal resistance within the motor stator. Increasing the thermal conductivity of the resin and improving the resin's ability to bond the slot liner to the stator surface should reduce this thermal resistance.
- The 2012 LEAF power modules incorporate a dielectric pad to provide electrical isolation. The dielectric pad and associated TIM interfaces (on both sides of the dielectric pad) are found to provide the greatest thermal resistance in the LEAF power modules. Analysis indicates that the use of a more conventional power module design (e.g., power modules that incorporate metalized ceramics) can improve thermal performance. However, the LEAF design may offer cost and reliability benefits.
- FEA transient models of both the LEAF motor and power electronic thermal management systems were developed. Work is currently underway to understand heat loss distributions within each system. Heat loss information will be used as inputs into the transient models and used to compute component temperatures under drive-cycle operations.

- Tests have been initiated to measure the thermal performance of the 2014 Honda Accord power electronics thermal management system.

Nomenclature

A	area
k	thermal conductivity
Q	heat
Rth	thermal resistance
R"th	specific thermal resistance
T	temperature

Subscripts

j	junction
l	liquid
s	stator
w	windings (e.g., motor windings)

FY 2015 Presentations /Publications/Patents

1. Moreno, G.; Bennion, K.; Cousineau, E.; King, C. "Thermal Performance Benchmarking." Advanced Power Electronics and Electric Motors FY15 Kickoff Meeting, DOE VTO, Oak Ridge, TN, November 2014.
2. Moreno, G.; Bennion, K.; Cousineau, E.; King, C. "Thermal Performance Benchmarking." 2015 DOE VTO Annual Merit Review, Crystal City, VA, June 2015.
3. Moreno, G.; Bennion, K.; Cousineau, E.; King, C. "Thermal Performance Benchmarking." 2015 Presentation to the DOE Vehicle Technologies Office (VTO) Electrical and Electronics Technical Team, Southfield, MI, September 2015.

Acknowledgements

The author would like to acknowledge the support provided by Susan Rogers and Steven Boyd, Technology Development Managers for the EDT Program, Vehicle Technologies Office, U.S. Department of Energy Office of Energy Efficiency and Renewable Energy. The significant contributions of Kevin Bennion, Emily Cousineau, and Charles King are acknowledged.

References

1. Burress, T. "Benchmarking of Competitive Technologies." 2012. DOE VTO Annual Merit Review, Washington DC, May 2012.
2. Burress, T. "Benchmarking EV and HEV Technologies." 2015. DOE VTO Annual Merit Review, Crystal City, VA, June 2015.
3. Sato, Y.; Ishikawa, S.; Okubo, T.; Abe, M.; Tamai, T., 2011. "Development of High Response Motor and Inverter System for the Nissan LEAF Electric Vehicle." SAE Technical Paper.
4. Emily, C.; Bennion, K.; DeVoto, D., Mihalic, M., Narumanchi, S., 2015. "Characterization of Contact and Bulk Thermal Resistance of Laminations for Electric Machines" NREL Technical Report NREL/TP-5400-63887.

5. Bennion, K.; and Cousineau, J., 2012. “Sensitivity Analysis of Traction Drive Motor Cooling.” Paper presented at the IEEE Transportation Electrification Conference and expo, Dearborn, Michigan.
6. Matweb. “Aluminum 6061-T6; 6061-T651" Accessed August 7, 2015. http://www.matweb.com/search/DataSheet.aspx?MatGUID=1b8c06d0ca7c456694c7777d9e10be5b&ckck=1